

# Estimation of water diffusivity parameters on grape dynamic drying

Inês N. Ramos<sup>a</sup>, João M.R. Miranda<sup>b</sup>, Teresa R.S. Brandão<sup>a</sup>, Cristina L.M. Silva<sup>a,\*</sup>

<sup>a</sup>CBQF – Centro de Biotecnologia e Química Fina, Biotechnology School – Catholic University of Portugal, Rua Dr. António Bernardino de Almeida, 4200-072 Porto, Portugal

<sup>b</sup>Centro de Engenharia Biológica, Universidade do Minho, Campus de Gualtar, 4710-057 Braga, Portugal

## Keywords:

Dynamic convective drying

Water diffusivity

Grapes

Numerical modelling

## A B S T R A C T

A computer program was developed, aiming at estimating water diffusivity parameters in a dynamic drying process with grapes, assessing the predictability of corresponding non-isothermal drying curves. It numerically solves Fick's second law for a sphere, by explicit finite differences, in a shrinking system, with anisotropic properties and changing boundary conditions.

Experiments were performed in a pilot convective dryer, with simulated air conditions observed in a solar dryer, for modelling the process. The equivalent radius of grapes decreased 30% until the end of the process, stressing the need to include shrinkage in mass and heat transfer models. It was observed that macroscopic shrinkage reflects cellular shrinkage, if plotted versus the normalised water content. Diffusivity values ranged between  $1 \times 10^{-16}$  and  $1 \times 10^{-10}$  m<sup>2</sup>/s. The developed methodology yields very good prediction of dynamic drying curves.

## Introduction

The earliest records of fruit drying refer to sun drying of apples, grapes and apricots in Egypt in the third century BC (Brennan, 1994). The most used grape varieties for producing raisins are Thompson Seedless, Muscat of Alexandria and Black Corinth (Patil et al., 1995). Raisins are the third biggest utilisation of grapes, following wine and table grapes.

In food drying modelling and simulation, Fickian models are the most widely accepted (Mulet et al., 1989; Raghavan et al., 1995; García-Pérez et al., 2009; Janjai et al., 2010). There is no standard methodology for determination of moisture diffusivity, therefore experimental evaluation is still necessary. Due to foods complexity, theoretical predictions are not viable (Karathanos et al., 1990).

Classification of available diffusivity determination methods is difficult (Zogzas et al., 1994). Karathanos et al. (1990) divided them into three classes: analysis of the drying data, sorption kinetics and permeation methods; and separated the analysis of drying data in: the method of slopes, a computer optimisation method and the regular regime method. Zogzas et al. (1994) divided them into six groups: permeation methods, sorption kinetics, concentration-distance curves, simplified drying methods at constant or variable diffusivity (method of slopes), the regular regime technique and numerical methods. These latter authors also presented a list on reported studies of diffusivity determination methods, mainly on food materials.

Permeation methods are grounded on Fick's first law of diffusion, with the sample placed between two constant concentration sources of the diffusant, but the experimental setup may be difficult. In the sorption kinetics method (also known as half-time technique) developed by Crank (1975), the material is placed in a constant concentration source. The concentration-distance curves (or concentration profiles) may be based on specific experimental techniques and may also evaluate moisture diffusivity dependence. The simplified drying method or method of slopes was used by several authors due to its easy applicability, and may also be applied to variable moisture diffusivity. The regular regime method was developed by Schoeber (1976) and it requires successive interpolations and differentiations of drying data, being complex to use.

Regarding numerical methods, all the three approaches have been used in food drying: finite differences, finite elements and finite volumes. A summary on numerical methods developed for analysing heat/cooling processes of foods is listed in Wang and Sun (2003). Numerical methods perform better than analytical solutions with real situations, such as non-linear and anisotropic food properties, irregular shaped materials, shrinkage and changing boundary conditions (Wang and Sun, 2003).

The main objectives of this work were: (i) to compare grape microscopic and macroscopic shrinkage data and determine shrinkage coefficients; (ii) to develop a computer program aiming at estimating grape moisture diffusivity parameters by numerical solution of Fick's second law, with a non-isothermal drying pattern; and (iii) to assess the predictability of corresponding non-isothermal drying curves.

\* Corresponding author. Tel.: +351 22 5580058; fax: +351 22 5090351.

E-mail address: [clsilva@esb.ucp.pt](mailto:clsilva@esb.ucp.pt) (C.L.M. Silva).

## Nomenclature

$a$	half the major axis	$Sh$	Sherwood number
$a_w$	water activity, mathematically equal to RH	$t$	time (s)
$A_p$	projected area of drying product ( $m^2$ )	$T$	absolute temperature (K)
$A_s$	surface area of drying product ( $m^2$ )	$T_{ave}$	average experimental temperature (K)
$b$	half the minor axis	$v$	free-stream velocity (m/s)
$Bi_m$	Biot number of mass transfer	$V$	volume ( $m^3$ )
$C$	Guggenheim constant	$X$	estimated water content on dry basis ( $kg_{water} kg_{dry matter}^{-1}$ )
$Co, Ko$	constants	$X_e$	equilibrium water content ( $kg_{water} kg_{dry matter}^{-1}$ )
$D$	water diffusivity ( $m^2 s^{-1}$ )	$X_m$	water content on dry basis, corresponding to the monolayer value ( $kg_{water} kg_{dry matter}^{-1}$ )
$e$	eccentricity of the revolving ellipse	$X_R$	water content at the surface of the product ( $kg_{water} kg_{dry matter}^{-1}$ )
FD	Feret diameter	$X_{exp}$	average experimental water content on dry basis ( $kg_{water} kg_{dry matter}^{-1}$ )
$h_D$	convective mass transfer coefficient ( $m s^{-1}$ )	$\bar{X}$	average water content ( $kg_{water} kg_{dry matter}^{-1}$ )
$H_1$	heat of condensation of pure water vapour ( $J mol^{-1}$ )	$a', b', c', D_0$	model parameters
$H_m$	heat of sorption of the monolayer of water ( $J mol^{-1}$ )	$\Delta r$	space interval (m)
$H_q$	heat of sorption of the multilayers ( $J mol^{-1}$ )	$\Delta t$	time interval (s)
$i$	node	$\nu$	air kinematic viscosity ( $m^2/s$ )
$K$	factor correcting properties of the multilayer molecules with respect to the bulk liquid	$\mu$	air dynamic viscosity ( $kg/m s$ )
$L$	length of the plate (m)	$\rho$	air density ( $kg/m^3$ )
$n$	number of experimental observations	<b>Subscripts</b>	
$nnodes$	total number of nodes	0	initial value
$ntimes$	total number of experimental points	$i$	at node $i$
$p$	number of parameters in a model	<b>Superscript</b>	
$r$	direction through which diffusion occurs (m)	$t$	at time $t$
$R$	equivalent radius		
$Re_L$	Reynolds number		
$R_g$	universal gas constant ( $J mol^{-1} K^{-1}$ )		
$R^2$	coefficient of determination		
RH	relative humidity (%)		
$s$	standard deviation of the experimental error		
Sc	Shmidt number		

## Materials and methods

### Description of grape samples

Fresh grapes from the Muscatel cultivar (Douro region, Portugal), were purchased in the Porto supplier market and stored in a refrigeration chamber (Fitoclima model D1200PH, Aralab, S. Domingos de Rana, Portugal) at 4 °C and 80% RH, for 2 months maximum. Fruits were visually selected from different clusters, to have similar size and maturity level, and no wounds. Peduncles were removed and berries were blanched in a pilot plant equipment (Armfield, Ringwood, England) in hot water at 99 °C during 15 s. Initial water content of grapes was gravimetrically measured by the AOAC – 984.25 method and water content during drying was mathematically calculated. Grapes dimensions were determined with a digital vernier caliper (Mitutoyo Digimatic model, Andover, England) in the longitudinal, vertical and equatorial directions.

### The drying experiments

This study was carried out in a pilot plant convective tray drier (Armfield UOP8, Ringwood, England) with forced air and controlled temperature and velocity (Fig. 1). Efforts were made to improve the convective drier in order to enable on-line acquisition of total weight, air temperature and relative humidity. Upstream and downstream of the drying trays, two air humidity probes and two thermocouples were placed. Air temperature and relative humidity values were recorded every 5 min in a squirrel datalogger (Grant Instruments 1023, Cambridge, England). Air humidity probes and thermocouples wires were both supplied by Grant Instruments.

Four experiments were performed: two for determining physical properties (experiments 1 and 2) and two for modelling the process with acquisition of mass (experiments 3 and 4). In the first two, samples with 10 berries each were taken daily from the drier. Mass acquisition was performed every 15 min for the last two experiments. In order to simulate air conditions observed in a solar dryer, located at Mirandela (region in the North of Portugal), experiments were carried out at 45 °C and ambient air relative humidity during the day (9 h), while during the night the heater was turned off and ambient temperature and air relative humidity were attained. Air velocity was set at 0.60 m/s and measured regularly with a vane anemometer (Airflow LCA 6000, Buckinghamshire, England).

### Image acquisition and image analysis

Grape shrinkage was determined with a video microscope (Olympus OVM 1000 NM, Tokyo, Japan) with a magnification of 9×. Two images were acquired, for each of the 10 berries of daily samples from the drying experiments 1 and 2. Images picture the larger and smaller faces of the berry. Calibration of length was performed with a stainless steel ruler. This technique is similar to the one used by Prado et al. (2000), with the exception that these authors used a camera fixed on a tripod. The equipment is composed of a probe (Olympus OVM 1000 N, Tokyo, Japan), a NTSC-PAL signal converter (Perfect Image DVT-87 BNC, Miami, USA), a colour video monitor (Sony Triniton PVM-1440 QM, Tokyo, Japan) and a PC, where images were also visualised and saved using Global Lab Image 3.0 (Data Translation, Marlboro, USA) software.

Grape images were analysed with Paint Shop Pro 4.12 and UTH-SCA Image Tool 2.0 softwares (University of Texas Health Science

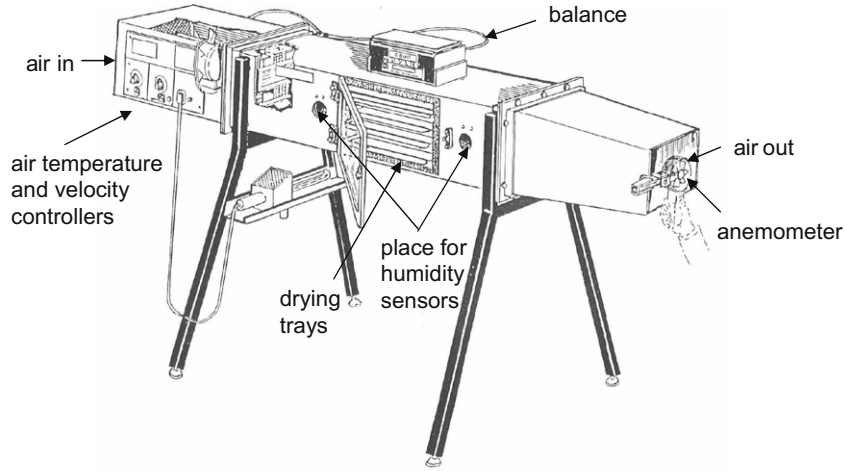


Fig. 1. Scheme of the pilot plant tray drier.

Center, Texas, USA). The geometrical features: area, perimeter, major and minor axis length, Feret diameter, elongation, roundness and compactness were determined. The definition of these parameters may be found in Ramos et al. (2004).

#### 2.4. Macroscopic shrinkage calculation

The surface area ( $A_s$ ) was calculated assuming that grape berries are ellipsoids, particularly prolate spheroids ("pointy" instead of "squashed", somewhat egg-shaped), for sake of simplicity, by the following mathematical equation (<http://home.att.net/~numerical/answer/geometry.htm>):

$$A_s = 2\pi b^2 + 2\pi \frac{ab}{e} \arcsin e \quad (1)$$

where  $a$  is half the major axis,  $b$  is half the minor axis and  $e$  is the eccentricity of the revolving ellipse (Eq. (2)).

$$e = \frac{\sqrt{a^2 - b^2}}{a} \quad (2)$$

$A_p$  is the projected area of berries, which may lay in any direction and was computed through Eq. (3) using the equivalent radius ( $R$ ).

$$A_p = \pi R^2 \quad (3)$$

The average equivalent radius of grapes was calculated using Eq. (4), where  $FD$  is the Feret diameter

$$R = \sqrt[3]{\left(\frac{FD}{2}\right)^2 b} \quad (4)$$

This methodology has the advantage of including the Feret diameter, taking into account wrinkles formation, which deviate grapes from the ellipsoidal shape; instead of using only the major and minor axis length.

$R$ ,  $A_s$  and  $A_p$  were related to the experimental average water content ( $X_{exp}$ ) by a simple linear relation, and the shrinkage parameters were obtained (Eqs (23)–(25)).

#### Mass transfer considerations

In order to analyse internal and external resistances to mass transfer, the Biot number of mass transfer ( $Bi_m$ ) was calculated (Geankoplis, 1983):

$$Bi_m = \frac{h_D V / A_s}{D} \quad (5)$$

$h_D$  is the convective mass transfer coefficient,  $V/A_s$  is the volume per surface ratio and  $D$  is water diffusivity inside the solid. This dimensionless number gives the ratio of the mass transfer rate at the interface per mass transfer rate in the interior of the solid (or ratio of the resistance to diffusion in the solid per resistance to convection in the fluid).

The bed of grapes was assumed to act as a flat plate for convection purposes, being the Reynolds number ( $Re_L$ ) and Schmidt number ( $Sc$ ) (Eqs. (6) and (7), respectively) calculated with the air conditions observed in the experiments.

$$Re_L = \frac{\rho v L}{\mu} = \frac{v L}{\nu} \quad (6)$$

$$Sc = \frac{\mu}{\rho D} \quad (7)$$

where  $\rho$  is the air density ( $\text{kg/m}^3$ ),  $v$  the free-stream velocity ( $\text{m/s}$ ),  $\nu$  the air kinematic viscosity ( $\text{m}^2/\text{s}$ ),  $L$  the plate length ( $\text{m}$ ), and  $\mu$  the air dynamic viscosity ( $\text{kg/m s}$ ). The length of the trays was 0.34 m.

$h_D$  was determined from a correlation with a dimensionless numbers (Eq. (8)) and a graph of evaporation from flat surfaces, both obtained from Coulson and Richardson (1965).

$$Sh = 0.037 Re_L^{0.8} Sc^{0.33} \quad (8)$$

being the Sherwood number:

$$Sh = \frac{h_D L}{D} \quad (9)$$

For the  $h_D$  calculation, average air conditions were used as well as a high water diffusivity value ( $1.5 \times 10^{-10} \text{ m}^2/\text{s}$ ) (the worst case scenario).

#### Estimation of diffusivity parameters

A computer program (SIMPFD.FOR) was developed in Fortran 77 language (Fortran 5.1, Microsoft Corporation®, 1990) aiming at estimating water diffusivity parameters in a dynamic drying process. Input data of the computer program are: experimental time and corresponding average water content (experiments 3 and 4), air temperature and relative humidity, shrinkage parameters and coefficients of sorption–desorption isotherms (Eq. (20)). Output data are diffusivity parameters. A schematic flowsheet of the computer program is presented in Fig. 2.

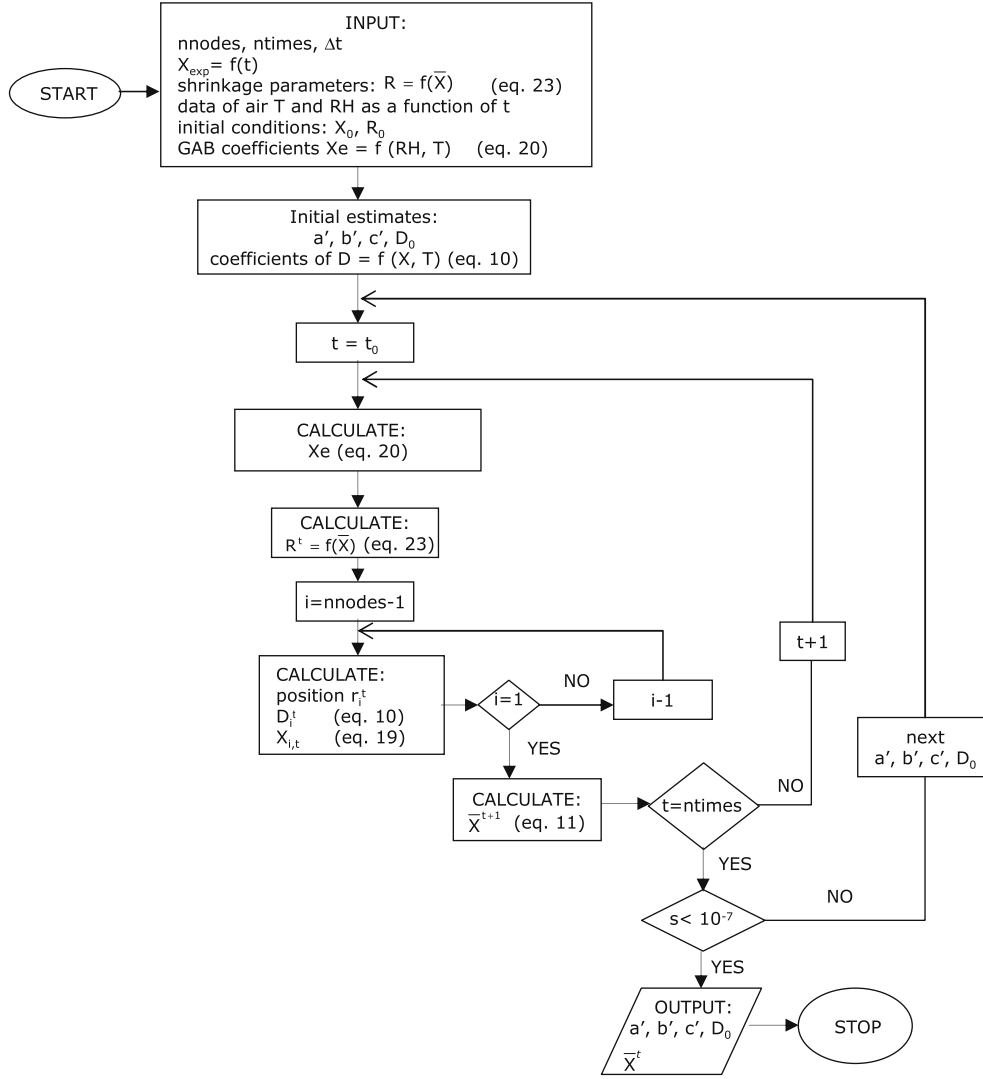


Fig. 2. Schematic flowsheet of the computer program SIMPFD.FOR for estimation of water diffusivity parameters in a dynamic drying process.

Our system presents shrinkage, anisotropic properties and changing boundary conditions. The computer program solves numerically Fick's second law for a sphere, by explicit finite differences method, with a total of twenty nodal points (see Section 2.7). It considers diffusivity dependence on water content and temperature (Eq. (10)) along drying and within grapes (non-isotropic characteristics). This equation was developed and is based on the one proposed by Mulet et al. (1989), but including a parabolic behaviour for the water content effect, instead of a linear effect. Water content was normalised, allowing a clear comparison between experiments. Any other available model can also be used in the computer program.

$$D = D_0 \exp \left[ a' \frac{X}{X_{exp0}} - b' \left( \frac{X}{X_{exp0}} \right)^2 - c' \left( \frac{1}{T} - \frac{1}{T_{ave}} \right) \right] \quad (10)$$

where  $D$  is the water diffusivity ( $\text{m}^2 \text{s}^{-1}$ ),  $X$  the water content on dry basis ( $\text{kg}_{\text{water}} \text{kg}_{\text{dry matter}}^{-1}$ ),  $X_0$  the initial average water content,  $T$  the absolute temperature (K),  $T_{ave}$  the average experimental temperature and  $a'$ ,  $b'$ ,  $c'$  and  $D_0$  are model parameters.  $T_{ave}$  was set at 303.15 K. The average predicted water content ( $\bar{X}$ ) was calculated for the entire product by the trapezoidal rule (Eq. (11)), in order to determine the standard deviation of the experimental error ( $s$ ) (Eq. (12)) (Box et al., 1978).

$$\bar{X} = \frac{\int X_i dV}{V} = \frac{\sum_{i=1}^{nnodes-1} \frac{(X_{i+1} + X_i)}{2} \frac{4}{3} \pi (r_{i+1}^3 - r_i^3)}{\frac{4}{3} \pi R^3} \quad (11)$$

where  $i$  is the node,  $V$  the volume ( $\text{m}^3$ ),  $r$  the direction through which diffusion occurs (m),  $R$  the equivalent radius of the sphere (m) and  $t$  is time (s).

$$s = \sqrt{\frac{\sum (X_{exp} - \bar{X})^2}{n - p}} \quad (12)$$

where  $n$  is the number of experimental observations and  $p$  the number of model parameters.

Parameters were estimated by non-linear regression analysis, and the Simplex algorithm (Nelder-Mead) was used for the least squares function minimisation. The statistical indicators, standard deviation of the experimental error ( $s$ ) and coefficient of determination ( $R^2$ ) were obtained.

#### Numerical solution of Fick's second law

Fick's second law was solved by the explicit finite differences method, as already referred. Developing the radius partial derivative in Fick's equation yields:

$$\frac{\partial X}{\partial t} = D \frac{\partial^2 X}{\partial r^2} + \frac{1}{r^2} \frac{\partial X}{\partial r} \frac{\partial (Dr^2)}{\partial r} \quad (13)$$

If one states

$$\frac{1}{r^2} \frac{\partial (Dr^2)}{\partial r} = F \quad (14)$$

and discretises partial derivatives (forward differences for discretisation of the time first derivative, and central differences for the space first derivative):

$$\frac{\partial X}{\partial t} = \frac{X_i^{t+1} - X_i^t}{\Delta t} \quad (15)$$

$$\frac{\partial X}{\partial r} = \frac{X_{i+1}^t - X_{i-1}^t}{2\Delta r} \quad (16)$$

$$\frac{\partial^2 X}{\partial r^2} = \frac{X_{i+1}^t - 2X_i^t + X_{i-1}^t}{\Delta r^2} \quad (17)$$

$$F_i^t = \frac{1}{r_i^2} \frac{D_{i+1}^t r_{i+1}^2 - D_{i-1}^t r_{i-1}^2}{2\Delta r} \quad (18)$$

where  $\Delta t$  is the time interval and  $\Delta r$  the space interval. Algebraic manipulation results in the following equation:

$$X_i^{t+1} = X_i^t \left( 1 - 2 \frac{\Delta t D_i^t}{\Delta r^2} \right) + X_{i+1}^t \left( \frac{\Delta t D_i^t}{\Delta r^2} + \frac{\Delta t F_i^t}{2\Delta r} \right) + X_{i-1}^t \left( \frac{\Delta t D_i^t}{\Delta r^2} - \frac{\Delta t F_i^t}{2\Delta r} \right) \quad (19)$$

It was assumed: (i) homogeneity of the water content inside the sphere at the beginning of the drying process, (ii) water content at the surface of the product ( $X_R$ ) always in equilibrium with surrounding air, and (iii) a symmetric condition at the centre of the sphere. The following boundary conditions can be written, with external dimension (equivalent radius) changing with time, as fruit shrinks:

- (i)  $t = 0, \quad 0 \geq r \geq R \quad X = X_0$
- (ii)  $t \leq 0, \quad r = R(t) \quad X_R = X_e(t)$
- (iii)  $t \leq 0, \quad r = 0, \quad \frac{\partial X}{\partial r} = 0$

where  $X_e$  is the equilibrium water content.

At the centre of the grape, distance between nodes one and two was set half of the distance for other nodal points, at every drying time.

Water content at the surface (last node –  $X_R$ ) was always assumed in equilibrium with changing air conditions, and was determined using the G.A.B. model (Eq. (20)):

$$\frac{X_e}{X_m} = \frac{CKa_w}{(1 - Ka_w)(1 - Ka_w + CKa_w)} \quad (20)$$

where  $X_m$  is the water content on dry basis, corresponding to the monolayer value,  $a_w$  the water activity,  $C$  the Guggenheim constant, and  $K$  a factor correcting properties of the multilayer molecules with respect to the bulk liquid (Bizot, 1983).  $C$  and  $K$  reflect the temperature effect:

$$C = C_0 \exp \left( \frac{H_1 - H_m}{Rg T} \right) \quad (21)$$

$$K = K_0 \exp \left( \frac{H_1 - H_q}{Rg T} \right) \quad (22)$$

where  $C_0$  and  $K_0$  are constants,  $H_1$  is the heat of condensation of pure water vapour ( $\text{J mol}^{-1}$ ),  $H_m$  the heat of sorption of the monolayer of water, and  $H_q$  is the heat of sorption of the multilayers. The Guggenheim–Anderson–deBoer model was recommended by the European project COST 90 on Physical Properties of Foods (Maroulis et al., 1988).

**Table 1**

G.A.B. model coefficients for Muscatel raisins, determined by Vázquez et al. (1999).

$X_m$	$C_0$	$(H_1 - H_m)/Rg$	$K_0$	$(H_1 - H_q)/Rg$
0.119	0.107	0.107	0.911	9.07

G.A.B. model coefficients were obtained from Vázquez et al. (1999) for Muscatel raisins (Table 1).

## Results and discussion

The mass transfer Biot number ( $Bi_m$ –Eq. (5)) ranged between 100 and 92, which undoubtedly indicates negligible resistance to external mass transfer.

The grapes average initial diameter, measured with the digital vernier calliper, was  $1.94 \pm 0.26$  cm. Blanched grapes presented water contents of  $77 \pm 1$  and  $78 \pm 1\%$  (on wet basis) for experiments 3 and 4, respectively.

### Comparing macroscopic and cellular shrinkage

Based on data from experiments 1 and 2, shrinkage equations were obtained (Eqs. (23)–(25)) for the average equivalent radius ( $R$ ), surface area ( $A_s$ ) and projected area ( $A_p$ ).

$$R = R_0 \left( 0.3654 \frac{\bar{X}}{X_{exp0}} + 0.6288 \right) \quad (23)$$

$$A_p = A_{p0} \left( 0.6314 \frac{\bar{X}}{X_{exp0}} + 0.3521 \right) \quad (24)$$

$$A_s = A_{s0} \left( 0.5627 \frac{\bar{X}}{X_{exp0}} + 0.4054 \right) \quad (25)$$

During the experiments, the equivalent radius of grapes ( $R$ ) decreased 30% until the end of the drying process. This significant variation stresses the need to include shrinkage in mass and heat transfer models.

In order to compare macroscopic and cellular shrinkage, data from a previous work (Ramos et al., 2004), of two replicates at  $30^\circ\text{C}$ , were used. Cellular shrinkage is described by the Feret diameter shrinkage, which is mathematically equivalent to radius shrinkage ( $FD/FD_0 = R/R_0$ ).

It was found that if plotted versus the normalized water content ( $X/X_0$ ), macroscopic and cellular shrinkage are extremely similar, as

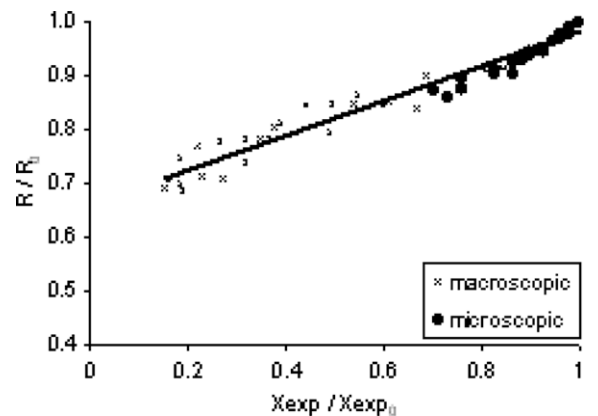


**Fig. 3.** Comparing macroscopic and cellular shrinkage.



observed in Fig. 3. This indicates that macroscopic shrinkage reflects cellular shrinkage.

#### Observed air conditions

Air conditions in a solar dryer were simulated inducing steps in air parameters, by changes in the heater of the convective dryer. The variation of air parameters (temperature and relative humidity) inside the convective drier is exemplified in Fig. 4. These sudden changes are square-wave profiles, somewhat different from the kind of sinusoidal variation observed in a solar dryer.

Air temperature and humidity data as a function of time were directly introduced into the SIMPFD.FOR program.

#### Estimated diffusivity parameters and predicted drying curves

Estimated diffusivity parameters of Eq. (10), calculated using SIMPFD.FOR computer program, and statistical indicators of corresponding predicted drying curves are presented in Table 2. Values regarding corresponding diffusivity (calculated from Eq. (10)) ranged from  $1 \times 10^{-16}$  to  $1 \times 10^{-10} \text{ m}^2/\text{s}$ , for temperatures between 20 and 50 °C and for water content values observed throughout the entire drying process. The lowest values correspond to the initial phase of the drying process, when water content is high, and for the lowest temperature values studied. The upper value lies within the range of diffusivities reported for fruits and vegetables by Ratti and Mujumdar (1996) and Gekas (1992). The calculated values are also in very good agreement with reported literature data for the particular case of raisins (Riva and Peri, 1983; Lomauro et al., 1985; Raghavan et al., 1995; Azzouz et al., 2002). However, the authors Riva and Peri (1983) and Lomauro et al. (1985) did not consider water content dependent diffusivity and determined

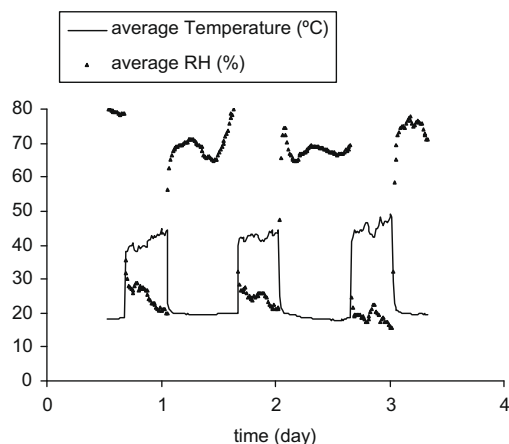


Fig. 4. Example of air temperature and relative humidity inside the convective dryer (experiment 3).

Table 2  
Estimated diffusivity parameters of Eq. (10) and statistical indicators.

Parameter	Estimate	
	Experiment 3	Experiment 4
$D_0 \times 10^{12} (\text{m}^2 \text{s}^{-1})$	1.75	2.93
$\hat{a}$	18.3	14.5
$\hat{b}$	32.7	27.1
$\hat{c}$ (K)	6870	6290
$R^2$	0.9833	0.9921
$s$	0.1054	0.0869

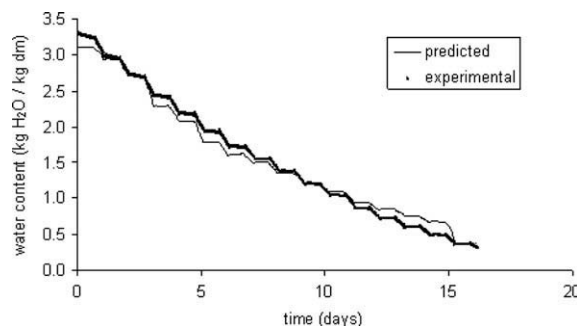


Fig. 5. Predicted drying curve (experiment 3).

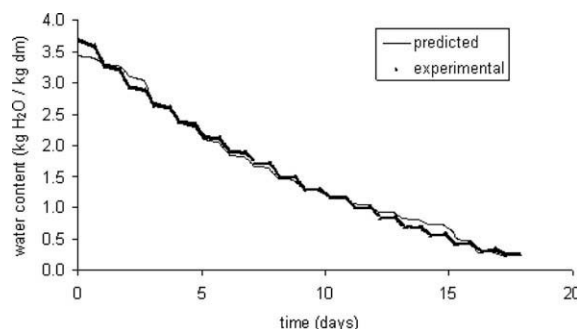


Fig. 6. Predicted drying curve (experiment 4).

a single value for the entire drying process, hence, these data are difficult to compare.

Reflecting the temperature effect, the  $c'$  parameter in Eq. (10) may be compared to the  $E_a/R$  term in the Arrhenius law, although lacking the physical meaning of the activation energy. Calculating corresponding activation energies from the  $c'$  parameter, the values of 57.1 and 52.3 kJ/mol were obtained for experiments 3 and 4, respectively. These values are in the same range of those found in literature, even if they are slightly higher than the ones determined by Riva and Peri (1983) and Simal et al. (1996) for grapes submitted to pre-treatments.

Predicted drying curves of experiments 3 and 4 are presented in Figs. 5 and 6, respectively. A good prediction was achieved for both experiments, as confirmed by  $R^2$  and  $s$  values (Table 2), notwithstanding some fitting discrepancies at the beginning and at the end of drying. These may be attributable to drying phenomena not accounted for in the diffusional model, and also to not considering shape variation and wrinkles formation. Although accounting for shrinkage, the computer program uses Fick's second law for a drying sphere, but grapes form wrinkles during drying and become elongated (ellipsoid). The solution for this would be the development of a tri-dimensional model.

One should be aware concerning collinearity of estimated diffusivity parameters. Since the model used was a four-parameter equation (Eq. (10)), diffusivity parameters interdependence would certainly occur. This means that different parameters values may lead to similar residuals of the least-squares estimation, which might compromise parameters' accuracy (in relation to their real values).

Overall, one can conclude that the methodology developed in this chapter yields very good prediction of dynamic drying curves.

#### Conclusion

The equivalent radius of grapes decreased 30% until the end of the drying process. This significant variation stresses the need to include shrinkage in mass and heat transfer models. Comparing

plots of macroscopic and microscopic shrinkage one may conclude that they are very similar. This indicates that macroscopic shrinkage reflects cellular shrinkage, if plotted versus the normalized water content ( $X/X_0$ ).

Estimation of diffusivity parameters, with the computer program, allowed the calculation of corresponding diffusivities values, which ranged between  $1 \times 10^{-16}$  and  $1 \times 10^{-10}$  m<sup>2</sup>/s. The values of 57.1 and 52.3 kJ/mol were obtained for the activation energies calculated from the  $c'$  parameter. These values were in the same range of those found in literature, even if they were slightly higher than the ones determined by Riva and Peri (1983) and Simal et al. (1996) for grapes submitted to pre-treatments.

A good prediction of drying curves was achieved for both experiments, as confirmed by  $R^2$  and  $s$  values, despite some fitting discrepancies at the beginning and at the end of drying. Overall, one can conclude that the developed methodology yields very good prediction of dynamic drying curves, although compromising diffusivity parameters' accuracy.

## Acknowledgements

The authors Inês N. Ramos and Teresa R.S. Brandão would like to acknowledge, respectively, PRAXIS XXI PhD Grant No. 18543/98 and Post-Doctoral Grant SFRH/BPD/11580/2002, to Fundação para a Ciência e a Tecnologia, Portugal.

## References

- Azzouz, S., Guizani, A., Jomaa, W., Belghith, A., 2002. Moisture diffusivity and drying kinetic equation of convective drying of grapes. *Journal of Food Engineering* 55, 323–330.
- Bizot, H., 1983. Using the 'G.A.B.' model to construct sorption isotherms. In: Jowitt, R., Escher, F., Hallström, B., Meffert, H., Spiess, W., Vos, G. (Eds.), *Physical Properties of Foods*. Applied Science Publishers, Essex, pp. 43–54.
- Box, G.E.P., Hunter, W.G., Hunter, J.S., 1978. *Statistics for experimenters: An introduction to design, data analysis, and model building*. New York, John Wiley and Sons.
- Brennan, J.G., 1994. *Food dehydration: A dictionary and guide*. Butterworth-Heinemann Ltd, Oxford.
- Coulson, J.M., Richardson, J.F., 1965. *Tecnologia química - Fluxo de fluidos, transferência de calor e transferência de massa*, second ed. Fundação Calouste Gulbenkian, London.
- Crank, J., 1975. *The mathematics of diffusion*, second ed. Clarendon Press, Oxford.
- García-Pérez, J.V., Carcel, J.A., García-Alvarado, M.A., Mulet, A., 2009. Simulation of grape stalk deep-bed drying. *Journal of Food Engineering* 90, 308–314.
- Geankoplis, C.J., 1983. *Transport processes and unit operations*, second ed. Allyn and Bacon, Boston.
- Gekas, V., 1992. *Transport phenomena of foods and biological material*. CRC Press, Boca Raton.
- Janjai, S., Mahayothee, B., Lamlet, N., Bala, B.K., Precoppe, M., Nagle, M., Muller, J., 2010. Diffusivity, shrinkage and simulated drying of litchi fruit (*Litchi Chinensis* Sonn). *Journal of Food Engineering* 96 (2), 214–221.
- Karathanos, V.T., Villalobos, G., Saravacos, G.D., 1990. Comparison of two methods of estimation of the effective moisture diffusivity from drying data. *Journal of Food Science* 55 (1), 218–223, 231.
- Lomauro, C.J., Bakshi, A.S., Labuza, T.P., 1985. Moisture transport properties of dry and semimoist foods. *Journal of Food Science* 50, 397–400.
- Maroulis, Z.B., Tsami, E., Marinou-Kouris, D., Saravacos, G.D., 1988. Application of the GAB model to the moisture sorption isotherms for dried fruits. *Journal of Food Engineering* 7, 63–78.
- Mulet, A., Berna, A., Rosselló, C., 1989. Drying of carrots I. Drying models. *Drying Technology* 7 (3), 537–557.
- Patil, V.K., Chakrawar, V.R., Narwadkar, P.R., Shinde, G.S., 1995. Grape. In: Salunkhe, D.K., Kadam, S.S. (Eds.), *Handbook of food science and technology*. Marcel Dekker Inc., New York, pp. 7–38.
- Prado, M.E.T., Alonso, L.F.T., Park, K.J., 2000. Shrinkage of dates (*Phoenix dactylifera* L.) during drying. *Drying Technology* 18 (1–2), 295–310.
- Raghavan, G.S.V., Tulasidas, T.N., Sablani, S.S., Ramaswamy, H.S., 1995. A method of determination of concentration dependent effective moisture diffusivity. *Drying Technology* 13 (5–7), 1477–1488.
- Ramos, I.N., Silva, C.L.M., Sereno, A.M., Aguilera, J.M., 2004. Quantification of microstructural changes during first stage air drying of grape tissue. *Journal of Food Engineering* 62 (2), 159–164.
- Ratti, C., Mujumdar, A.S., 1996. Drying of fruits. In: Somogyi, L.P., Ramaswamy, H.S., Hui, Y.H. (Eds.), *Processing fruits: Science and technology*. Technomic Publishing, Lancaster, pp. 185–220.
- Riva, M., Peri, C., 1983. Étude du séchage des raisins. 1- effect de traitements de modification de la surface sur la cinétique du séchage. *Sciences des Aliments* 3, 527–550.
- Schoeber, W.J.A.H., 1976. *Regular regimes in sorption processes*. The Netherlands, Eindhoven University of Technology.
- Simal, S., Mulet, A., Catalá, P.J., Cañellas, J., Rosselló, C., 1996. Moving boundary model for simulating moisture movement in grapes. *Journal of Food Science* 61 (1), 157–160.
- Vázquez, G., Chenlo, F., Moreira, R., Carballo, L., 1999. Desorption isotherms of muscatel and aledo grapes, and the influence of pre-treatments on muscatel isotherms. *Journal of Food Engineering* 39, 409–414.
- Wang, L., Sun, D., 2003. Recent developments in numerical modelling of heating and cooling processes in the food industry - a review. *Trends in Food Science and Technology* 14, 408–423.
- Zogzas, N.P., Maroulis, Z.B., Marinou-Kouris, D., 1994. Densities, shrinkage and porosity of some vegetables during air drying. *Drying Technology* 12 (7), 1653–1666. </http://home.att.net/~numérica/answer/geometry.html/>.